

Kondo resonance enhanced supercurrent in single wall carbon nanotube Josephson junctions

K Grove-Rasmussen* and H Ingerslev Jørgensen and P E Lindelof

*Nano-Science Center, Niels Bohr Institute,
University of Copenhagen, Denmark*

Abstract

We have contacted single wall carbon nanotubes grown by chemical vapor deposition to superconducting Ti/Al/Ti electrodes. The device, we here report on is in the Kondo regime exhibiting a four-fold shell structure, where a clear signature of the superconducting electrodes is observed below the critical temperature. Multiple Andreev reflections are revealed by sub-gap structure and a narrow peak in the differential conductance around zero bias is seen depending on the shell filling. We interpret the peak as a proximity induced supercurrent and examine its interplay with Kondo resonances.

*Electronic address: k'grove@fys.ku.dk

I. INTRODUCTION

Single wall carbon nanotubes (SWCNT) have been under intense investigation for more than a decade due to their unique mechanical and electrical properties. They are one-dimensional conductors with two conducting modes and when contacted to electrodes they behave as quantum dots, where phenomena as Fabry-Perot interference [1], Kondo effect [2] and Coulomb blockade [3, 4] have been observed. The different regimes can be accessed by indirectly controlling the coupling between the SWCNT and the contacts by choice of contact material. In the low transparency regime (closed quantum dot), electron transport is blocked except at charge degeneracy points, where electrons can tunnel through the SWCNT only one by one due to Coulomb blockade. When the transparency is increased (intermediate regime) cotunneling of electrons becomes possible, which can give rise to the Kondo effect. Finally in the high transparency regime electrons on the SWCNT are not well defined and the phenomena observed (broad resonances) are due to interference of electron waves (Fabry-Perot interference). The possibility of contacting carbon nanotubes to superconducting leads [5, 6, 7, 8] opens up for the interesting study of effects related to superconductivity such as supercurrent and multiple Andreev reflections [9] together with the above mentioned phenomena. In the Fabry-Perot regime recent experiments have confirmed that the supercurrent is modulated by the quantized nature of the energy spectrum of the SWCNT, *i.e.*, a Josephson field effect transistor with only two modes [10, 11]. Experimental access to the less transparent regimes [12, 13, 14, 15] is even more interesting due to the possibility of probing the competition between effects related to Coulomb blockade and superconductivity. Coulomb blockade generally suppresses the supercurrent and interesting phenomena such as π -junction behavior has been observed in the closed quantum dot regime in nanowires [14]. For more transparent devices the supercurrent can be enhanced due to Kondo physics [16]. Both supercurrent and Kondo physics are two extensively studied manybody effects in condensed matter physics and SWCNT Josephson junctions thus give a unique possibility to examine their interplay. The supercurrent is predicted to coexist with Kondo resonances provided that the Kondo related energy scale $k_B T_K$ is bigger than the superconducting energy gap Δ [16, 17, 18]. The importance of the ratio between these parameters has recently been addressed in different measurements [19]. In this article we extend this investigation to SWCNTs contacted to superconducting leads in order to experimentally probe the interplay

between supercurrent and Kondo physics. We investigate the gate dependence of a narrow zero bias conductance peak interpreted as a proximity induced supercurrent and show that the observation of a supercurrent in Kondo resonances depends on the ratio between the two energy scales ($k_B T_K/\Delta$) with a crossover close to 1 qualitatively consistent with theory.

II. EXPERIMENTAL DETAILS

SWCNTs are grown from catalyst islands consisting of Fe-oxide and Mo-oxide supported by aluminum nano-particles [20]. Growth is performed by chemical vapor deposition at 850 °C with a controlled flow of gasses Ar: 1 L/min, H₂: 0.1 L/min, CH₄: 0.5 L/min. During heating the furnace is kept under an Ar and H₂ flow, whereas cooling is done in Ar. We reduce cooling time by air-cooling the furnace. The substrate is a doped silicon wafer (used as back gate) with a 500 nm SiO₂ layer on top. Pairs of superconducting electrodes of Ti/Al/Ti (5/40/5 nm) are defined directly on top of the SWCNT by electron beam lithography followed by optical lithography to define the Cr/Au bonding pads. The first titanium layer of the metallic trilayer ensures good contact to the SWCNT, whereas the thicker middle aluminum layer is the actual superconductor in the device. Finally, the top layer of Ti is intended to stop oxidation of the aluminum. The gap between the source and drain electrode is typically around 0.5 μm. In the same evaporation process a four-probe device is made next to the S-SWCNT-S devices, which is used to measure the transition temperature $T_c = 760$ mK and the critical field around $B_c = 100$ mT of the superconductor. From Bardeen-Cooper-Schrieffer (BCS) theory we deduce the superconducting energy gap $\Delta = 1.75k_B T_c = 115$ μeV. The devices are cooled in a ³He-⁴He dilution fridge with a base temperature around 30 mK and we use standard lock-in techniques.

III. SUB-GAP STRUCTURE AND SUPERCURRENT

At room temperature the current through the device is gate dependent, which reveals that the SWCNT is semiconducting. Figure 1(a) shows a bias spectroscopy plot at 30 mK of the SWCNT device in the Kondo regime. It is measured at negative gate voltages and thus transport takes place through the valence band, i.e., tunneling of holes. The superconductivity in the leads is suppressed by a relative weak magnetic field of 180 mT ($>B_c$).

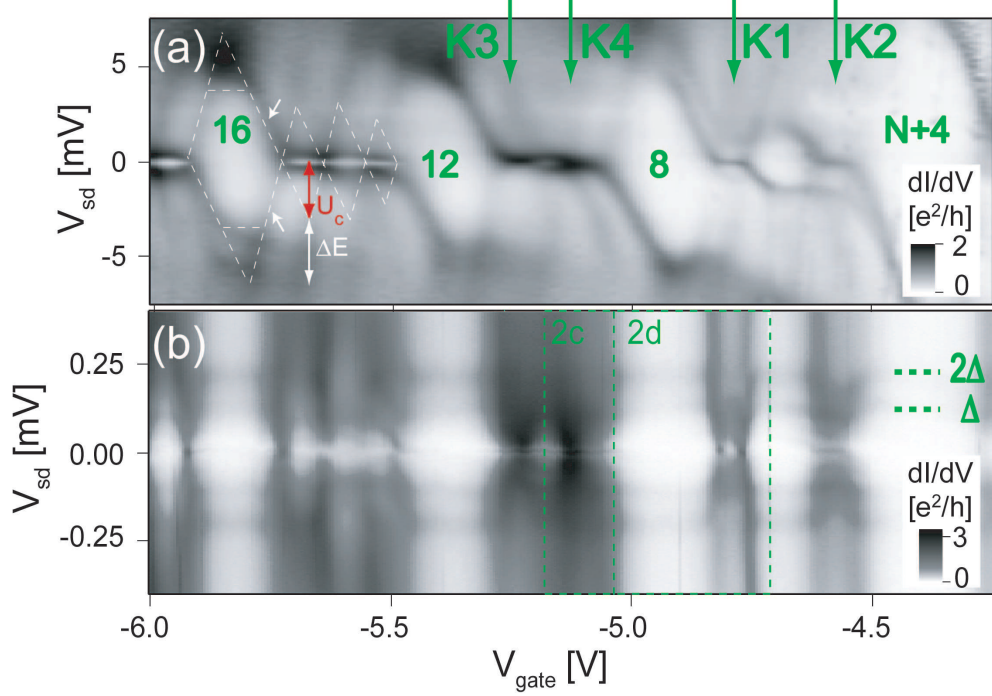


FIG. 1: (a) Bias spectroscopy plot of a SWCNT device at 30 mK showing a four-fold Coulomb blockade shell structure. The numbers indicate the additional hole filling, where big diamonds correspond to filled shells. Four Kondo resonances K1-K4 are identified. A magnetic field of 180 mT is applied to suppress superconductivity in the leads. (b) Bias spectroscopy plot for the same gate range as (a) but with the leads in the superconducting state. A sub-gap structure emerges, most clearly visible at $\pm\Delta/e$ and $\pm 2\Delta/e$ (horizontal green dashed lines). The green dashed rectangles are the gate voltage regions shown in Fig. 2(c) and 2(d).

The plot shows Coulomb blockade diamonds [21] with a characteristic pattern of three small diamonds followed by a bigger diamond as indicated with white lines for hole filling 13-16. Such Coulomb blockade diamond structure indicates a four-fold degenerate shell structure due to spin and orbital degrees of freedom, where each shell contains two spin-degenerate orbitals [22]. The filled shells corresponding to the big Coulomb blockade diamonds are marked in Fig. 1(a) by the additional number of holes on the SWCNT quantum dot. Due to intermediate transparency contacts significant cotunneling is allowed which tends to smear the features. The charging energy and the level spacing between the shells are estimated as half the source-drain height of the very faintly visible small diamonds and by the addi-

tional source-drain height of the big diamonds [23] giving $U_c \sim 3 \text{ meV}$ and $\Delta E \sim 4 \text{ meV}$, respectively (see arrows Fig. 1). A very rough estimate of the level broadening $\Gamma \sim 1 \text{ meV}$ and the asymmetry in the coupling to source and drain $\alpha = \Gamma_s/\Gamma_d \sim 0.4$ are extracted from the current plateaus at negative and positive bias (100 nA and -60 nA) at the white arrows. The current is modified due to the four-fold degeneracy which enhances the in-tunneling rate with 4 compared to the out-tunneling rate giving $(e/\hbar)4\Gamma_s\Gamma_d/(4\Gamma_s + \Gamma_d)$ and $(e/\hbar)(4\Gamma_d\Gamma_s/(\Gamma_s + 4\Gamma_d))$ for negative and positive bias polarity, respectively [24]. Furthermore, four Kondo resonances K1-K4 are identified (green arrows) and labeled in ascending order based on their Kondo temperatures. The Kondo temperatures are estimated by fitting the normal state conductance versus V_{sd} (solid line in Fig. 3a-b) to a Lorentzian line shape. The half width at half maximum of each Lorentzian fit yields the estimated Kondo temperature giving $T_K \sim 2 \text{ K}$, 4.5 K, 5 K and 6 K for K1-K4. For hole filling 13-15, conductance ridges at low finite bias are seen instead of zero bias Kondo resonances. The exact origin of these features are not fully understood, but they are attributed to inelastic cotunneling through two slightly split orbitals in the shell, which might include Kondo physics as well [25]. We note that these lines are not related to superconductivity.

Figure 1(b) shows a bias spectroscopy plot at low bias voltages for the same gate range as Fig. 1(a) with the leads in the superconducting state. A sub-gap structure clearly appears [9]. The peaks in differential conductance at $V_{sd} = \pm 2\Delta/e \sim \pm 230 \mu\text{V}$ are attributed to the onset of quasi-particle tunneling. At lower bias the transport is governed by Andreev reflections, which are possible due to the intermediate transparency between the SWCNT and the superconducting leads [26]. Features at biases $V_n = \pm 2\Delta/(en), n = 2, 3, \dots$ are expected due to the opening of higher order multiple Andreev reflection processes as the bias is lowered [27, 28]. Peaks at $V_{sd} = \pm\Delta/e \sim \pm 115 \mu\text{V}$ are clearly seen consistent with the energy gap found from BCS theory. Furthermore, for some ranges in gate voltage a narrow zero bias conductance peak is seen. We note, that this zero bias peak is visible in most of the Kondo resonances and is the subject to analysis below.

These above mentioned effects due to superconductivity are more clearly revealed in high resolution data shown in Fig. 2(c) and 2(d) corresponding to the green dashed rectangles in Fig. 1(b). Figure 2(a) and 2(b) show the same gate and bias regions as (c) and (d) with the leads in the normal state for comparison. Clearly the sub-gap structure is due to the proximity of the superconducting leads. The peaks at $\pm 2\Delta/e$ and $\pm\Delta/e$ are mostly

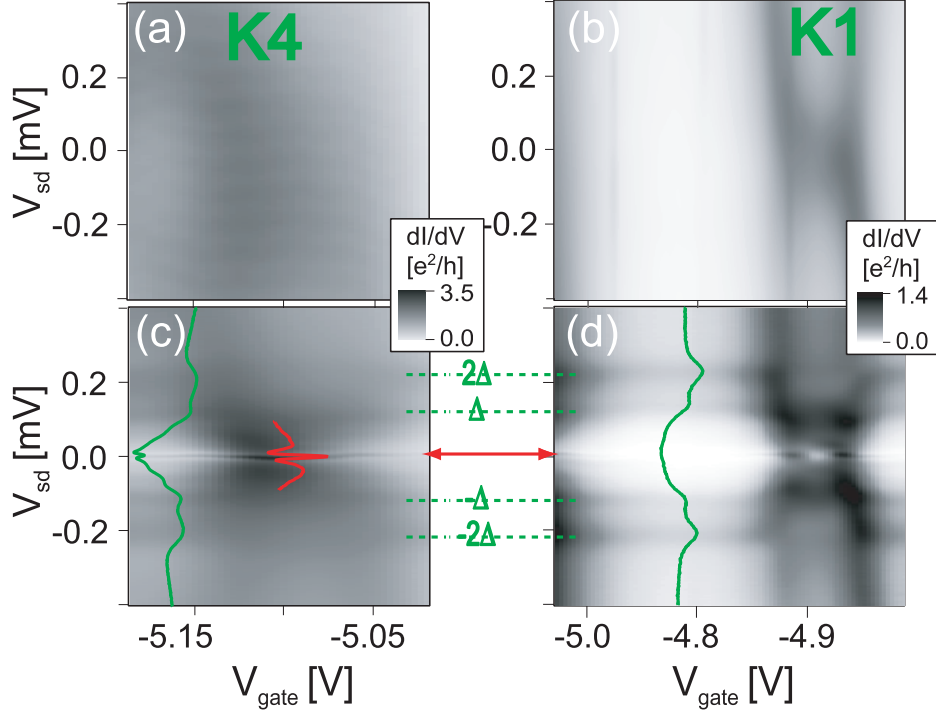


FIG. 2: (a-b) Bias spectroscopy plot at 30 mK with the leads in the normal state ($B = 180$ mT) for Kondo resonance K4 and K1, respectively. (c-d) High resolution data with the leads superconducting for the same gate and bias voltages as in the normal state above. The corresponding gate regions are shown by the dashed green rectangles in Fig. 1(b). A sub-gap structure appears at bias voltage $\pm 2\Delta/e$ and $\pm\Delta/e$ indicated by the green dashed lines. This is particularly clear in the Coulomb blockade region (d) and also seen in the green traces, which are dI/dV versus bias curves extracted from the plots. A zero bias conductance peak (red arrow) is also visible throughout Kondo resonance K4 as shown by the red trace in (d) and for some gate voltages in (c).

pronounced in the Coulomb blockade region as expected due to lower effective transparency [27] (d) while being more smeared in the high conducting region of K4 (c). Green curves show bias cuts, where higher order multiple Andreev reflection features are faintly visible in (c). A strong gate dependence of the sub-gap structure is observed when the gate voltage is tuned closer to the Coulomb resonances on each side of K1 from the Coulomb diamond with even occupation. This behavior has previously been observed [9] and explained by the interplay between multiple Andreev reflection and a resonant level [29, 30]. The zero bias conductance peak indicated by the red arrow is clearly visible in Kondo resonance K4 (red trace in (c)) and also present for some gate voltages in (d). Similar behavior of a zero bias peak in Kondo

resonances have been observed in other devices [13]. We interpret the zero bias conductance peak as being due to a proximity induced supercurrent running through the SWCNT. The magnitude of the supercurrent is estimated by the area of the peak giving a typical value in the order of $I_m \sim 0.2$ nA. A similar analysis of a zero bias conductance peak as supercurrent has successfully been carried out for an open quantum dot [11], *i.e.*, without Coulomb blockade effects. We note that an alternative interpretation of the origin of the zero bias peak based on quasiparticle current (multiple Andreev reflections) with a cut-off for higher order multiple Andreev reflection processes has also been suggested [31], but in this article the supercurrent interpretation will be pursued. The value of the measured supercurrent is highly suppressed compared to its theoretically expected value for one spin-degenerate level with the deduced asymmetric coupling ($\alpha = 0.4$) at resonance $I_0^{res} = 2e\Delta/\hbar (\Gamma_{min}/\Gamma) \sim 8$ nA in the broad resonance (short) regime $\Gamma > \Delta$, where $\Gamma_{min} = \min(\Gamma_s, \Gamma_d) \sim 0.3$ meV [32]. Despite having two spin-degenerate levels in the SWCNT, only one level is available due to Coulomb blockade.

The suppression is partly explained within an extended resistively and capacitively shunted junction model due to interaction of the SWCNT Josephson junction with its electrical environment. The electrical environment for this device is the low (serial) resistance between the Josephson junction and the bonding pads as well as the capacitance between the source and drain bonding pads via the backgate. The low serial resistance turns out to play a crucial role making the device an *underdamped* Josephson junction [10, 11, 33, 34]. This means that the full value of the critical current is never measured due to thermally activated phase-slips. A more intuitive understanding is obtained by the mechanical analog to the Josephson junction of a fictitious particle in a tilted washboard potential, where the tilt is given by the current and the phase difference between the superconductors is "running" as the fictitious particle moves in the potential. When the particle stays in a minimum of the washboard potential (constant phase), a supercurrent is seen. However, as the current increases the washboard potential is tilted and at the critical current the particle can slide into the next minimum. If thermal excitations are significant this process happens at lower current than the critical current. Since the junction is underdamped, the friction of the particle is low and it thus easily acquires a "run away" phase, that suppresses the supercurrent, which results in a much lower measured supercurrent. In contrast to the reported underdamped carbon nanotube Josephson junction in the Fabry-Perot regime [11], the effect of

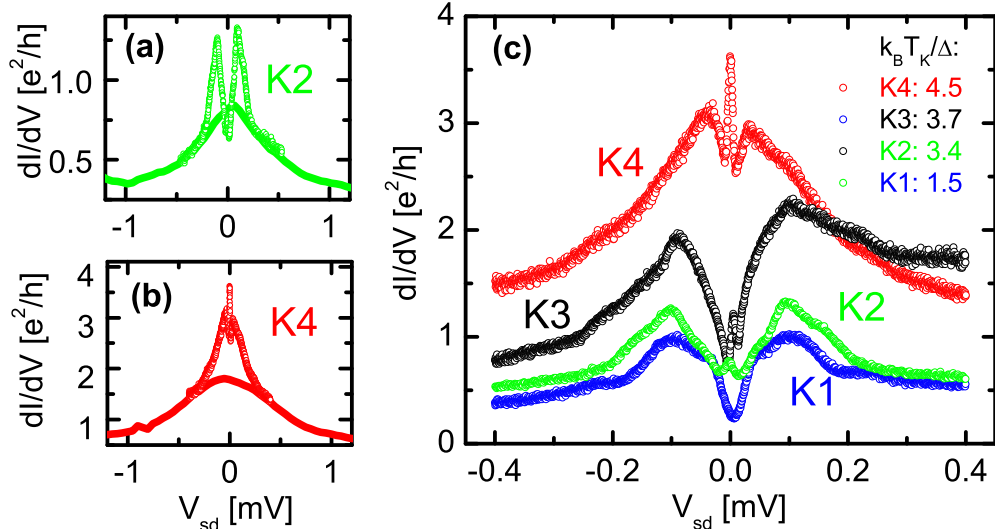


FIG. 3: dI/dV versus V_{sd} for Kondo resonances K1-K4 shown in Fig. 1(a) illustrating the effect of superconducting leads. (a-b) Solid lines and circles are with the leads in the normal and superconducting state, respectively. (c) The four Kondo resonances K1-K4 for small bias voltages with the leads in the superconducting state. The measured supercurrent given by the zero bias peak area is zero for the lowest value of the ratio $k_B T_K / \Delta$, while it increases as this ratio is increased.

Coulomb blockade and single hole tunneling also contribute to the suppression of the supercurrent, because Cooper pair transport is a two particle tunneling process. A quantitative analysis of the suppression due to Coulomb blockade is outside the scope of this article. This issue is being addressed in a separate work, where the on-chip electrical circuit of the SWCNT Josephson junction has been modified and the effects of Coulomb blockade thus can be compared to theoretical calculations [35]. Finally, we note that noise effects giving rise to thermally activated phase slips can be analyzed in the overdamped case [36].

IV. KONDO PHYSICS AND SUPERCURRENT

We now return to the Kondo resonances K1-K4 and analyze the interplay between Kondo physics and supercurrent. The solid curves in Fig. 3(a) and 3(b) show bias cuts with the leads in the normal state through the center of Kondo resonance K2 and K4, respectively (see Fig. 1(a)). The circles correspond to the behavior when the leads are superconducting. In both cases an enhancement of the differential conductance is observed for bias voltages between

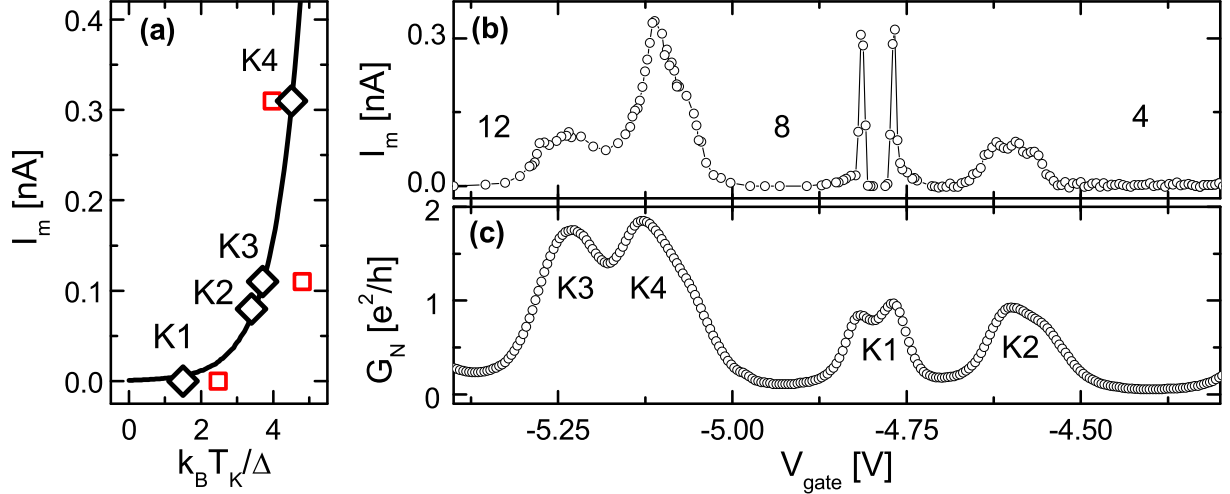


FIG. 4: (a) The measured supercurrent is zero for K1 and shown to increase as a function of $k_B T_K / \Delta$ (K1-K4). An exponential fit to the data points is given by the solid curve as guideline, where the Kondo temperature is based on the width of the resonance (black diamonds). The red squares are the Kondo temperature obtained from the temperature dependence (K1, K3 and K4). (b) Measured supercurrent versus gate voltage in the range with the Kondo resonances K1-K4, where the additional hole number is given for filled shells as in Fig. 1(a). A finite supercurrent is seen in the center of the broader Kondo resonance K2, while being zero in the center of narrowest Kondo resonance K1. This behavior does not reflect the normal state conductance G_N shown for the same gate range below in (c).

$\pm 2\Delta/e$ and a zero bias conductance peak is present due to supercurrent. The measured supercurrent is largest for the Kondo resonance with the highest Kondo temperature (K4), *i.e.*, broadest Kondo resonance. In Fig. 3(c) bias sweeps at the center of all four Kondo resonances are shown with the leads in the superconducting state. The Kondo temperature normalized by the superconducting energy gap ($k_B T_K / \Delta$) is the important parameter and is given for each resonance in the figure. It is seen that the measured supercurrent vanishes for the lowest ratio (blue circles) while it emerges and increases as the ratio is increased. The crossover is close to $k_B T_K / \Delta \sim 1$.

To illustrate this point more clearly, the measured supercurrent versus $k_B T_K / \Delta$ is plotted in Fig. 4(a) for the four Kondo resonances analyzed above (black diamonds). The solid curve shows a guideline to the eye based on an exponential fit to the available data points. The overall trend is qualitative consistent with existing theory, which predicts a suppression of

the supercurrent in the so-called weak coupling regime ($k_B T_K \ll \Delta$), while the supercurrent coexists with Kondo resonances in the strong coupling regime ($k_B T_K \gg \Delta$) [17, 18]. The red squares show the measured supercurrent where the Kondo temperature is extracted from the temperature dependence for completeness (only data available for K1, K3 and K4) [37].

Finally, Fig. 4(b) shows the measured supercurrent as a function of gate voltage in the range including the four Kondo resonances. It is strongly gate dependent illustrating effects of the four Kondo resonances. Figure 4(c) shows the zero bias conductance G_N with the leads in the normal state for the same gate range. The supercurrent *does not* directly reflect the normal state conductance G_N as in the case of an open quantum dot [10, 11], where the supercurrent is uniquely determined by the normal state conductance. This is most clearly seen by comparing Kondo resonance K1 and K2. No supercurrent is present in the center of the Kondo resonance K1 despite the high normal state conductance, while a finite supercurrent is present in Kondo resonance K2 with equally high normal state conductance in contrast to the behavior expected in the open quantum dot regime. Similarly, the Kondo resonances K3 and K4 have almost the same normal state conductances, but very different measured supercurrent. These observations support the above analysis that the interplay between Kondo physics and superconductivity has the fraction $k_B T_K / \Delta$ as the important parameter for the observation of supercurrent in Kondo resonances, i.e., the bias width of the Kondo resonances and not only their normal state conductance is important. We also note that the measured supercurrent in diamond 4, 8 and 12 is zero due to Coulomb blockade. The supercurrent in the high T_K Kondo resonances can thus be viewed as being enhanced from the suppressed values by Coulomb blockade and the single spin due to the formation of Kondo resonances. Furthermore, the overall behavior of the supercurrent of these four Kondo resonances also indirectly indicates a π to 0 transition of the current phase relation of the Josephson junction as a function of the parameter $k_B T_K / \Delta$ [17,18]. Similar gate voltage behavior has been observed in Ref. [15], but the authors do not show the magnitude of the supercurrent as a function of Kondo temperature. We end by noting that for large Kondo temperatures compared to the superconducting energy gap (K4), the observed gate voltage dependence of the supercurrent resembles the behavior of a superconducting single electron transistor, i.e., the supercurrent obtains a sharp maximum at the gate voltage corresponding to the center of the odd diamond [38].

V. CONCLUSION

In conclusion SWCNTs have been contacted to superconducting Ti/Al/Ti leads creating SWCNT Josephson junctions. We observe sub-gap structure due to multiple Andreev reflections and a narrow zero bias conductance peak. The zero bias peak is interpreted as a proximity induced supercurrent with a suppressed magnitude due to the underdamped nature of the Josephson junction and Coulomb blockade. We examine its interplay with Kondo resonances and the measured supercurrent is shown to coexist with Kondo resonances which have high Kondo temperatures compared to the superconducting energy gap, while being suppressed when the Kondo temperatures becomes comparable with the superconducting energy gap, qualitative consistent with existing theory.

Acknowledgement

We like to thank Karsten Flensberg, Tomáš Novotný and Jens Paaske for fruitful discussions. Furthermore, we wish to acknowledge the support of the Danish Technical Research Council (The Nanomagnetism framework program), EU-STREP Ultra-1D and CARDEQ programs.

References

-
- [1] W. Liang, M. Bockrath, D. Bozovic, J. H. Hafner, M. Tinkham, and H. Park. Fabry - Perot interference in a nanotube electron waveguide. *Nature*, 411:665, 2001.
 - [2] J. Nygård, D. H. Cobden, and P. E. Lindelof. Kondo physics in carbon nanotubes. *Nature*, 408:342, 2000.
 - [3] S. J. Tans, M. H. Devoret, H. Dai, A. Thess, R. E. Smalley, L. J. Geerligs, and C. Dekker. Individual single-wall carbon nanotubes as quantum wires. *Nature*, 386:474, 1997.
 - [4] M. Bockrath, D. Cobden, P. McEuen, N. Chopra, A. Zettl, A. Thess, and R. Smalley. Single Electron Transport in Ropes of Carbon Nanotubes. *Science*, 275:1922, 1997.

- [5] A. Y. Kasumov, R. Deblock, M. Kociak, B. Reulet, H. Bouchiat, I. I. Khodos, Y. B. Gorbatov, V. T. Volkov, C. Journet, and M. Burghard. Supercurrents Through Single-Walled Carbon Nanotubes. *Science*, 284:1508, 1999.
- [6] A. F. Morpurgo, J. Kong, C. M. Marcus, and H. Dai. Gate-Controlled Superconducting Proximity Effect in Carbon Nanotubes. *Science*, 286:263, 1999.
- [7] V. Krstić, S. Roth, M. Burghard, J. Weis, and K. Kern. Suppression of superconductor quasiparticle tunneling into single-walled carbon nanotubes. *Phys. Rev. B*, 68(20):205402, 2003.
- [8] J. Haruyama, K. Takazawa, S. Miyadai, A. Takeda, N. Hori, I. Takesue, Y. Kanda, T. Akazaki, and H. Takayanagi. Supercurrent in diffusive multi-walled carbon nanotubes. *Physica C Superconductivity*, 408:85–87, 2004.
- [9] M. R. Buitelaar, W. Belzig, T. Nussbaumer, B. Babić, C. Bruder, and C. Schönenberger. Multiple Andreev Reflections in a Carbon Nanotube Quantum Dot. *Phys. Rev. Lett.*, 91(5):057005, 2003.
- [10] P. Jarillo-Herrero, J. A. van Dam, and L. P. Kouwenhoven. Quantum supercurrent transistors in carbon nanotubes. *Nature*, 439:953, 2006.
- [11] H. I. Jørgensen, K. Grove-Rasmussen, T. Novotný, K. Flensberg, and P. E. Lindelof. Electron Transport in Single-Wall Carbon Nanotube Weak Links in the Fabry-Perot Regime. *Phys. Rev. Lett.*, 96:207003, 2006.
- [12] D. C. Ralph, C. T. Black, and M. Tinkham. Spectroscopic Measurements of Discrete Electronic States in Single Metal Particles. *Phys. Rev. Lett.*, 74:3241, 1995.
- [13] K. Grove-Rasmussen, H. I. Jørgensen, and P. E. Lindelof. Single Wall Carbon Nanotube Weak Links. In *Proceedings of the International Symposium on Mesoscopic Superconductivity and Spintronics 2006*. To be published by World Scientific Publishing, 2006.
- [14] J. A. van Dam, Y. V. Nazarov, E. P. A. M. Bakkers, S. De Franceschi, and L. P. Kouwenhoven. Supercurrent reversal in quantum dots. *Nature*, 442:667, 2006.
- [15] J.-P. Cleuziou, W. Wernsdorfer, V. Bouchiat, T. Ondarçuhu, and M. Monthieux. Carbon nanotube superconducting quantum interference device. *Nature Nanotechnology*, 1:53, 2006.
- [16] L. I. Glazman and K. A. Matveev. Resonant Josephson current through Kondo impurities in a tunnel barrier. *Journal of Experimental and Theoretical Physics Letters*, 49:659, 1989.
- [17] F. Siano and R. Egger. Josephson Current through a Nanoscale Magnetic Quantum Dot.

- Phys. Rev. Lett.*, 93(4):047002, 2004.
- [18] M.-S. Choi, M. Lee, K. Kang, and W. Belzig. Kondo effect and Josephson current through a quantum dot between two superconductors. *Phys. Rev. B*, 70(2):020502(R), 2004.
- [19] M. R. Buitelaar, T. Nussbaumer, and C. Schönenberger. Quantum Dot in the Kondo Regime Coupled to Superconductors. *Phys. Rev. Lett.*, 89(25):256801, 2002.
- [20] J. Kong, H. T. Soh, A. M. Cassell, C. F. Quate, and H. Dai. Synthesis of individual single-walled carbon nanotubes on patterned silicon wafers. *Nature*, 395:878, 1998.
- [21] L. P. Kouwenhoven, C. M. Marcus, P. E. McEuen, S. Tarucha, R. M. Westervelt, and N.S. Wingreen. Mesoscopic Electron Transport. pages 105–214. Kluwer Academic Publishers, 1997.
- [22] S. Sapmaz, P. Jarillo-Herrero, J. Kong, C. Dekker, L. P. Kouwenhoven, and H. S. J. van der Zant. Electronic excitation spectrum of metallic carbon nanotubes. *Phys. Rev. B*, 71(15):153402, 2005.
- [23] S. De Franceschi, S. Sasaki, J. M. Elzerman, W. G. van der Wiel, S. Tarucha, and L. P. Kouwenhoven. Electron Cotunneling in a Semiconductor Quantum Dot. *Phys. Rev. Lett.*, 86:878, 2001.
- [24] B. Babić, T. Kontos, and C. Schönenberger. Kondo effect in carbon nanotubes at half filling. *Phys. Rev. B*, 70(23):235419, 2004.
- [25] J. Paaske, A. Rosch, P. Wolfle, N. Mason, C. M. Marcus, and J. Nygård. Nonequilibrium Singlet-Triplet Kondo Effect in Carbon Nanotubes. *Nature Physics*, 2:460, 2006.
- [26] A.F.Andreev. *Zh. Eksp Theor. Fiz.*, 46:1823, 1964.
- [27] T. M. Klapwijk, G. E. Blonder, and M. Tinkham. *Physica B+C*, 109-110:1657, 1982.
- [28] E. N. Bratus', V. S. Shumeiko, and G. Wendin. Theory of Subharmonic Gap Structure in Superconducting Mesoscopic Tunnel Contacts. *Phys. Rev. Lett.*, 74:2110, March 1995.
- [29] A. L. Yeyati, J. C. Cuevas, A. López-Dávalos, and A. Martín-Rodero. Resonant tunneling through a small quantum dot coupled to superconducting leads. *Phys. Rev. B*, 55:R6137, 1997.
- [30] G. Johansson, E. N. Bratus, V. S. Shumeiko, and G. Wendin. Resonant multiple Andreev reflections in mesoscopic superconducting junctions. *Phys. Rev. B*, 60:1382–1393, 1999.
- [31] E. Vecino, M. R. Buitelaar, A. Martin-Rodero, C. Schönenberger, and A. Levi Yeyati. Conductance properties of nanotubes coupled to superconducting leads: Signatures of Andreev states dynamics. *Solid State Comm.*, 131:625, 2004.

- [32] C. W. J. Beenakker. Three "universal" mesoscopic Josephson effects. *ArXiv Condensed Matter e-prints*, 2004.
- [33] A. Steinbach, P. Joyez, A. Cottet, D. Esteve, M. H. Devoret, M. E. Huber, and J. M. Martinis. Direct Measurement of the Josephson Supercurrent in an Ultrasmall Josephson Junction. *Physical Review Letters*, 87(13):137003, September 2001.
- [34] D. Vion, M. Götz, P. Joyez, D. Esteve, and M. H. Devoret. Thermal Activation above a Dissipation Barrier: Switching of a Small Josephson Junction. *Phys. Rev. Lett.*, 77:3435, 1996.
- [35] H. I. Jørgensen, T. Novotný, K. Grove-Rasmussen, K. Flensberg, and P. E. Lindelof. *To be published*.
- [36] V. Ambegaokar and B. I. Halperin. Voltage Due to Thermal Noise in the dc Josephson Effect. *Phys. Rev. Lett.*, 23:274, August 1969.
- [37] D. Goldhaber-Gordon, H. Shtrikman, D. Mahalu, D. Abusch-Magder, U. Meirav, and M. A. Kastner. Kondo effect in a single-electron transistor. *Nature*, 391:156, 1998.
- [38] P. Joyez, P. Lafarge, A. Filipe, D. Esteve, and M. H. Devoret. Observation of parity-induced suppression of Josephson tunneling in the superconducting single electron transistor. *Phys. Rev. Lett.*, 72:2458, 1994.